

## Patterned Growth of Large Oriented Organic Semiconductor Single Crystals on Self-Assembled Monolayer Templates

Alejandro L. Briseno,<sup>†</sup> Joanna Aizenberg,<sup>\*,‡</sup> Yong-Jin. Han,<sup>‡</sup> Rebecca A. Penkala,<sup>‡</sup> Hyunsik Moon,<sup>‡</sup> Andrew J. Lovinger,<sup>‡</sup> Christian Kloc,<sup>‡</sup> and Zhenan Bao<sup>\*,§</sup>

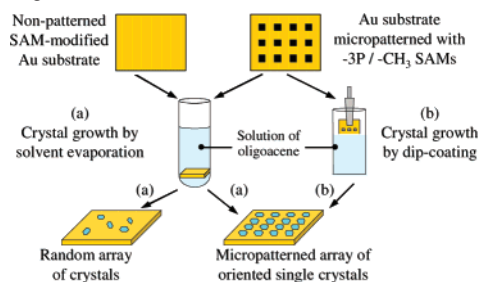
Department of Chemistry and Biochemistry, University of California—Los Angeles, Los Angeles, California 90095, Bell Laboratories, Lucent Technologies, Murray Hill, New Jersey 07974, and the Department of Chemical Engineering, Stanford University, Stanford, California 94305

Received May 4, 2005; E-mail: zbao@chemeng.stanford.edu; jaizenberg@lucent.com

There has been a recent surge of interest in the fabrication of electronic devices from high quality single crystals of organic semiconductors.<sup>1,2</sup> The importance of using the single crystals stems from the fact that intrinsic charge transport properties can be probed due to the lack of grain boundaries and molecular disorder<sup>1</sup>—the defects commonly present in polycrystalline organic thin films.<sup>3</sup> Such defects cause low mobilities and, therefore, reduce the performance of organic thin film transistors (OTFTs). In contrast, mobilities as high as 20 cm<sup>2</sup>/Vs have been reported for single-crystal rubrene transistors.<sup>2c</sup> Despite the high mobilities reported for single-crystal devices, there are many factors limiting their applications. In addition to the difficulties of fabricating good electrical contacts on single crystals, the most challenging task is handling the fragile crystals. Currently, single crystals are hand-picked and made into an individual device, but this method is impractical for fabricating a high density of devices over a large area. Our long-term goal is to understand the growth behavior of organic semiconductors in order to selectively grow oriented single-crystalline organic semiconductors in designated locations directly in a device structure. In this communication, we report a method for inducing site-specific growth of large oriented organic semiconductor crystals using micropatterned self-assembled monolayers (SAMs) bearing the regions of oligophenylene thiols as nucleation templates.

Controlling the nucleation sites, sizes, and orientation of organic semiconductor single crystals remains a challenge. Recently, a number of new crystallization strategies have emerged, in which specially designed organic substrates are used to control crystallization.<sup>4</sup> Particularly promising crystallization templates are SAMs of functionalized thiols supported on metal films that demonstrate the ability to promote the nucleation and growth of inorganic crystals with finely tuned crystal sizes, crystallographic orientation, and crystal micropatterning.<sup>5</sup> The use of SAMs as templates for organic crystallization is, however, more limited. In the latter case, selective nucleation would likely rely on van der Waals interactions instead of ionic interactions critical at the organic–inorganic interface. This type of interaction at the SAM–organic crystal interface has been recently demonstrated to control oriented growth of molecular crystals.<sup>6</sup> It has also been shown that by using patterned SAM templates, site-specific crystallization of organic charge-transfer salts<sup>7a</sup> and selective deposition of pentacene films<sup>7b,c</sup> could be achieved. The growth of large pentacene single crystals with sizes up to 100 μm was induced by silicon surfaces modified with a monolayer of cyclohexene molecules.<sup>8</sup> The control over multiple parameters of semiconductor crystal growth (i.e., orientation, pattern, and crystal sizes) in one system has not yet been achieved.

**Scheme 1.** Schematic Illustration of the Experimental Procedure for the SAM-Induced Growth of Organic Semiconductor Crystals from an Oligoacene/THF Solution<sup>10</sup>



With this goal in mind, we first examined the ability of various SAM-modified gold substrates to template the formation of organic semiconductor crystals. Oligoacene molecules were chosen for crystal growth studies since they have been recently reported to exhibit single-crystal field-effect.<sup>2a,b,9</sup> Substrates modified with SAMs of alkanethiols bearing methyl, amine, and carboxylic acid end groups, as well as with monolayers of thiophenol, biphenylthiol, and terphenylthiol (further referred to as  $-\text{CH}_3$ ,  $-\text{NH}_2$ ,  $-\text{CO}_2\text{H}$ ,  $-\text{P}$ ,  $-\text{2P}$ ,  $-\text{3P}$ , respectively) were immersed in a saturated anthracene/THF solution and allowed to evaporate over several days (Scheme 1a).<sup>10</sup> The nucleation density and surface coverage (%) of organic semiconductor crystals were analyzed for at least 10 individual samples of each SAM.

The results showed that the nucleation density of anthracene crystals formed on different SAMs increases in the following order:  $-\text{CH}_3 < -\text{NH}_2 < -\text{CO}_2\text{H} < \text{bare gold} < -\text{P} < -\text{2P} < -\text{3P}$ , with the surface coverage of  $1.0 \pm 1$ ,  $1.9 \pm 1$ ,  $2.4 \pm 1$ ,  $3.0 \pm 1$ ,  $3.2 \pm 2$ ,  $6.3 \pm 2$ , and  $23 \pm 6$ , respectively.<sup>10</sup> Anthracene crystals grown on  $-\text{3P}$  SAMs exhibit uniform facet angles,  $\delta_1$  and  $\delta_2$ , when viewed down the surface normal (Figure 1a). Their X-ray diffraction pattern showed only the (001) anthracene reflection and its second-order peak.<sup>10</sup> Computer simulation of the morphology of an anthracene crystal nucleated from the (001) plane and the corresponding angles  $\delta_1$  and  $\delta_2$  (Figure 1b) perfectly matched those of the grown crystals. In this orientation, the anthracene molecules are tilted by an angle of  $\sim 26^\circ$  from the surface normal, similar to the  $27^\circ$  tilt of the molecules in the  $-\text{3P}$  SAM (Figure 1c),<sup>11</sup> and the intermolecular distance in the crystal's  $a$ -axis direction has an exact lattice match to the underlying  $-\text{3P}$  SAM in the next-nearest-neighbor direction (Figure 1c,d). These data show that the  $-\text{3P}$  SAM matches the molecules' orientation and the packing of the nascent anthracene crystal in the  $c^*$ -direction, thus providing a nearly perfect template for the oriented nucleation of the anthracene crystals from the (001) plane. The ability to control the orientation of organic semiconductor crystals is highly desirable since the

<sup>†</sup> University of California—Los Angeles.

<sup>‡</sup> Lucent Technologies.

<sup>§</sup> Stanford University.

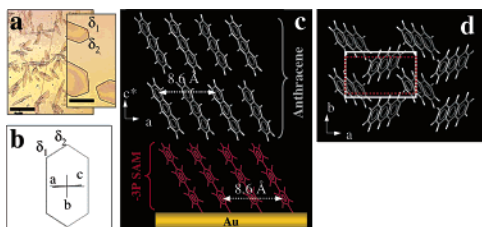


**Figure 1.** Oriented growth of anthracene on a  $-3P$  SAM. (a) Optical micrographs of anthracene crystals grown on a nonpatterned SAM by solvent evaporation;<sup>10</sup> scale bar =  $100\ \mu\text{m}$ . Inset: High-magnification image of single crystals showing the interfacial angles  $\delta_1$  and  $\delta_2$  analyzed in the morphological study ( $\delta_1 = 125.8 \pm 2.6^\circ$ ,  $\delta_2 = 109.7 \pm 4.0^\circ$ ); scale bar =  $10\ \mu\text{m}$ . (b) Computer simulation of the morphology of an anthracene crystal nucleated from the (001) plane ( $\delta_1 = 125^\circ$ ,  $\delta_2 = 110^\circ$ ). (c and d) Molecular modeling of the (001)-oriented anthracene crystal on the  $-3P$  SAM, viewed along the surface (c) and down the surface normal (d) (solid line shows the unit cell of the crystal; red dotted line shows the unit cell of the SAM).

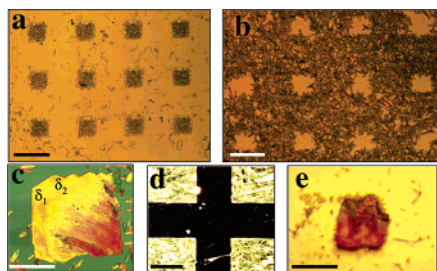


**Figure 2.** Optical micrographs of patterned arrays of anthracene crystals grown on micropatterned SAMs. (a)  $-3P$  squares in the  $-CH_3$  background; scale bar =  $300\ \mu\text{m}$ . (b)  $-CH_3$  squares in the background of  $-3P$ ; scale bar =  $300\ \mu\text{m}$ . (c) Large oriented single crystal of anthracene overgrowing the entire underlying  $100 \times 100\ \mu\text{m}$  square region of  $-3P$ ; scale bar =  $50\ \mu\text{m}$ . Method: solvent evaporation. (d) Patterned anthracene crystalline films formed by dip-coating.<sup>10</sup> Note the highly resolved edge in the pattern; scale bar =  $300\ \mu\text{m}$ . (e) Single crystal of 5-chlorotetracene grown by dip-coating, occupying an entire  $100 \times 100\ \mu\text{m}$  domain of the  $-3P$  SAM.

charge carrier mobility in a single crystal can vary along different crystallographic planes.<sup>1</sup>

Having demonstrated that the  $-3P$  SAM is an effective template for oriented crystallization of organic semiconductors, we then addressed the possibility of controlling the location and the pattern of nucleation. To achieve a better selectivity of patterned growth, we designed the template with SAMs, which showed two extremes in their templating activity:  $-CH_3$  and  $-3P$ . Micropatterned substrates with regions of  $-3P$  and  $-CH_3$  having different geometries and relative sizes were made by microcontact printing ( $\mu\text{CP}$ ).<sup>5a,b,10</sup> These substrates were then placed in a saturated anthracene/THF solution, where subsequent crystal growth occurred by solvent evaporation at an average rate of  $2\ \text{mL}$  per day over a period of several days (Scheme 1a).<sup>10</sup> As expected, highly localized crystal growth onto oligophenylene thiol-patterned regions was observed (Figure 2a–c). Alternatively, dip-coating has also been used (Scheme 1b)<sup>10</sup> to achieve selective crystallization of organic semiconductor molecules (Figure 2d,e). Surface coverage of crystals grown on micropatterned  $-3P$  regions increased to  $>95\%$  (Figure 2) versus  $23\%$  for the nonpatterned  $-3P$  substrates (Figure 1a). Significantly, we were able to grow large single crystals often occupying the whole  $-3P$  region up to  $100 \times 100\ \mu\text{m}$  in size (Figure 2c,e).

While we have yet to thoroughly construe the mechanism for selective crystallization, our results suggest that site-specific interactions between the semiconductor molecules and the oligophenylene SAMs may arise from  $\pi$ -interactions, which play important roles in facilitating the oriented nucleation of organic semiconductor crystals. The SAM of  $-3P$  can be regarded as a 2D crystalline layer of oriented molecules that are chemically similar

to the nucleating organic semiconductor. As such, the oligophenylene-modified regions may act as surrogate crystal surfaces for the nascent organic crystal and thus provide sites for effective heteroepitaxy. For templates patterned with  $-3P$  and  $-CH_3$ , the flux of molecules to the growing crystals in the  $-3P$  region will induce near-surface concentration gradients and deplete anthracene molecules from the less active alkylthiol areas.<sup>10</sup> As a result, increased surface coverage and highly selective, patterned growth of oriented semiconductor single crystals are observed. Similar phenomena and its detailed mechanistic assessment have been reported for high-resolution growth of inorganic crystals on patterned SAM templates.<sup>5b</sup>

In conclusion, this work demonstrates that *oriented, patterned* growth of *large* organic semiconductor crystals can be achieved using SAMs micropatterned with regions of terphenylthiol as nucleation templates. The ability to control various aspects of crystal growth in one system provides a powerful technique for the bottom-up fabrication of organic single-crystal devices. Ongoing work at understanding the growth of organic semiconductors and optimizing the conditions to achieve patterned growth of oriented individual single crystals in selective regions over large areas for device applications are being pursued in our laboratory. Preliminary experiments show that functional transistors can be prepared with organic single crystals patterned in  $-3P$  regions. Further optimization of device structure and performance is needed and will be reported in due course.<sup>10</sup> By directly growing crystals onto devices, one can avoid handling fragile crystals.

**Acknowledgment.** A.L.B. acknowledges the Bell Labs Graduate Research Fellowship. Z.B. acknowledges partial financial support from the Finmeccanica Faculty Scholar Award, the 3M Faculty Award, and BASF Co. A.L.B. thanks Professor N. S. Lewis and Dr. B. S. Brunschwig for use of the MMRC at Caltech.

**Supporting Information Available:** Experimental conditions. This material is available free of charge via the Internet at <http://pubs.acs.org>.

## References

- (1) Sundar, V. C.; Zaumseil, J.; Podzorov, V.; Menard, E.; Willett, R. L.; Someya, T.; Gershenson, M. E.; Rogers, J. A. *Science* **2004**, *303*, 1644–1646 and references therein.
- (2) (a) Aleshin, A. N.; Lee, J. Y.; Chu, S. W.; Kim, J. S.; Park, Y. W. *Appl. Phys. Lett.* **2004**, *84*, 5383–5385. (b) Katz, H. E.; Kloc, Ch.; Sundar, V.; Zaumseil, J.; Briseno, A. L.; Bao, Z. *J. Mater. Res.* **2004**, *19*, 1995–1998. (c) Podzorov, V.; Menard, E.; Borissov, A.; Kiryukhin, V.; Rogers, J. A.; Gershenson, M. E. *Phys. Rev. Lett.* **2004**, *93*, 866021–866024.
- (3) (a) Ling, M. M.; Bao, Z. *Chem. Mater.* **2004**, *16*, 4824–4840. (b) Kelley, T. W.; Frisbie, C. D. *J. Phys. Chem. B* **2001**, *105*, 4538–4540.
- (4) (a) Addadi, L.; Weiner, S. *Proc. Natl. Acad. Sci. U.S.A.* **1985**, *82*, 4110–4113. (b) Mann, S. *Nature* **1993**, *365*, 499–505. (c) Berman, A.; Ahn, D. J.; Lio, A.; Salmemon, M.; Reichert, A.; Charych, D. *Science* **1995**, *269*, 515–518. (d) Stupp, S. I.; Braun, P. V. *Science* **1997**, *277*, 1242–1248. (e) Lee, S. W.; Lee, S. K.; Belcher, A. M. *Adv. Mater.* **2003**, *15*, 689–692.
- (5) (a) See review on SAMs: Love, J. C.; Estroff, L. A.; Kriebel, J. K.; Ralph G. Nuzzo, R. G.; Whitesides, G. M. *Chem. Rev.* **2005**, *105*, 1103–1170. (b) Aizenberg, J.; Black, A. J.; Whitesides, G. M. *Nature* **1999**, *398*, 495–498. (c) Han, Y.-J.; Aizenberg, J. *Angew. Chem., Int. Ed.* **2003**, *42*, 3668. (d) Travaille, A. M.; Kaptijn, L.; Verwer, P.; Hulsken, B.; Elemans, J. A. A. W.; Nolte, R. J. M.; van Kempen, H. *J. Am. Chem. Soc.* **2003**, *125*, 11571–11577. (e) Aizenberg, J. *Adv. Mater.* **2004**, *16*, 1295–1302.
- (6) (a) Hiremath, R.; Varney, S. W.; Swift, J. A. *Chem. Mater.* **2004**, *16*, 4948–4954. (b) Hu, W. S.; Tao, Y. T.; Hsu, Y. J.; Wei, D. H.; Wu, Y. S. *Langmuir* **2005**, *21*, 2260–2266.
- (7) (a) Noh, D.-Y.; Willing, G. A.; Han, C. Y.; Shin, K.-S.; Geiser, U.; Wang, H. H. *Chem. Mater.* **2004**, *16*, 4777–4782. (b) Steudel, S.; Janssen, D.; Verlaak, S.; Genoe, J.; Heremans, P. *Appl. Phys. Lett.* **2004**, *85*, 5550–5552. (c) Choi, H. Y.; Kim, S. H.; Jang, J. *Adv. Mater.* **2004**, *16*, 732–736.
- (8) Meyer zu Heringdorf, F.-J.; Reuter, M. C.; Tromp, R. M. *Nature* **2001**, *412*, 517–520.
- (9) Moon, H.; Zeis, R.; Borkent, E.-J.; Besnard, C.; Lovinger, A. J.; Siegrist, T.; Kloc, Ch.; Bao, Z. *J. Am. Chem. Soc.* **2004**, *126*, 15322–15323.
- (10) See Supporting Information for additional details and additional data.
- (11) Himmel, H.-J.; Terfort, A.; Woll, C. *J. Am. Chem. Soc.* **1998**, *120*, 12069–12074.

JA052919U